



Chemistry A European Journal

 **Chemistry
Europe**
European Chemical
Societies Publishing

Accepted Article

Title: 1- and 2-Photon Phototherapeutic Effects of Ru(II) Polypyridine Complexes in the Hypoxic Centre of Large Multicellular Tumour Spheroids and Tumour-Bearing Mice

Authors: Johannes Karges, Shi Kuang, Yih Ching Ong, Hui Chao, and Gilles Gasser

This manuscript has been accepted after peer review and appears as an Accepted Article online prior to editing, proofing, and formal publication of the final Version of Record (VoR). This work is currently citable by using the Digital Object Identifier (DOI) given below. The VoR will be published online in Early View as soon as possible and may be different to this Accepted Article as a result of editing. Readers should obtain the VoR from the journal website shown below when it is published to ensure accuracy of information. The authors are responsible for the content of this Accepted Article.

To be cited as: *Chem. Eur. J.* 10.1002/chem.202003486

Link to VoR: <https://doi.org/10.1002/chem.202003486>

WILEY-VCH

RESEARCH ARTICLE

1- and 2-Photon Phototherapeutic Effects of Ru(II) Polypyridine Complexes in the Hypoxic Centre of Large Multicellular Tumour Spheroids and Tumour-Bearing Mice

Johannes Karges,^[a] Shi Kuang,^[b] Yih Ching Ong,^[a] Hui Chao,^{*[b]} and Gilles Gasser^{*[a]}

Abstract: During the last decades, photodynamic therapy (PDT), an approved medical technique, has received increasing attention to treat certain types of cancer. Despite recent improvements, the treatment of large tumors remains a major clinical challenge due to the low ability of the photosensitizer (PS) to penetrate a 3D cellular architecture and the low oxygen concentrations present in the tumour centre. To mimic the conditions found in clinical tumors, exceptionally large 3D multicellular tumour spheroids (MCTSs) with a diameter of 800 μm were used in this work to test a series of new Ru(II) polypyridine complexes as 1-Photon and 2-Photon PSs. These metal complexes were found to fully penetrate the 3D cellular architecture and to generate singlet oxygen in the hypoxic centre upon light irradiation. While having no observed dark toxicity, the lead compound of this study showed an impressive phototoxicity upon clinically relevant 1-Photon (595 nm) or 2-Photon (800 nm) excitation with a full eradication of the hypoxic centre of the MCTSs. Importantly, this efficacy was also demonstrated on mice bearing an adenocarcinomic human alveolar basal epithelial tumour.

Introduction

Cancer has emerged as one of the deadliest diseases worldwide. Photodynamic Therapy (PDT) is a minimal invasive medical technique to treat this disease, often in combination with other methods (i.e., surgery, chemotherapy, radiation therapy or immunotherapy). In PDT, a preferably non-toxic photosensitizer (PS) is activated at a specific wavelength to generate reactive oxygen species (ROS). The majority of clinically approved PSs act by an energy transfer of the PS to molecular oxygen ($^3\text{O}_2$) to generate singlet oxygen ($^1\text{O}_2$). As ROS and $^1\text{O}_2$ are highly reactive, they can rapidly interact with their biological surroundings to trigger cell death.^[1] Despite recent research advances, the clinical applications of PDT remains sometimes unsatisfactory. Many tumours and especially large tumours show, after a PDT treatment, a regression of their outer spheres while their core remain intact, causing, after a certain time, a cancer relapse.^[2] This incomplete tumour eradication is due to several factors: 1)

the PS is not able to penetrate a 3D cellular architecture; 2) the oxygen concentration in the centre of the tumour is low (i.e., hypoxia), which is hampering the production of the therapeutically necessary ROS and $^1\text{O}_2$; 3) light is not delivered to the tumour centre.^[3] Consequently, there is a need for the evaluation of new PSs in large tumour models that can better simulate the conditions found in the tumours of patients.

Multicellular tumour spheroids (MCTSs) can mimic the pathological conditions found in clinically-relevant tumours. MCTSs with a diameter of 200 μm are frequently used to simulate 3D cell-cell as well as cell-matrix interactions. They can therefore be utilised to model the drug delivery of a compound.^[4] This is important since many investigated drug candidates have failed the translation from promising results in a 2D monolayer model to a 3D or an *in vivo* model due to compromised drug delivery.^[5] Furthermore, MCTSs are also able to simulate hypoxia and proliferation gradients to the centre. Since the vast majority of PDT agents act by an oxygen-dependent mechanism, the treatment of hypoxic tumors remains a major medical challenge.^[6] Despite these limitations, the successful treatment of the hypoxic regions of melanoma MCTSs with a diameter of 280 μm was recently reported.^[7] Studies have shown that the oxygen diffusion inside of MCTSs is limited to approximately 200 μm .^[8] Therefore, larger MCTS are able to generate a hypoxic core, which can better simulate the pathological conditions found in clinically-relevant tumours. Despite these benefits, studies of the antitumor effects of compounds in large MCTSs remain very rare.^[9] To overcome this limitation and promote a better understanding of the biological effects of new compounds, there is an urgent need for in-depth studies of the ability of new compounds in large MCTSs.

Ru(II) polypyridine complexes are gaining increasing attention as PDT PSs due to their attractive chemical and photophysical properties (e.g., high water solubility, chemical stability and photostability).^[10] Despite their remarkable characteristics, the majority of PSs are activated using either UV or blue light, limiting the light penetration inside the tissue and therefore their application to treat deep seated or large tumours. To overcome this limitation, there is a need for the development of Ru(II) polypyridine complexes with an absorption in the biological spectral window (600-900 nm).^[11] This aim could be achieved by a red-shift of the 1-Photon (1P) absorption or the use of a 2-Photon (2P) process, in which the compound absorbs two photons of low energy/high wavelengths simultaneously. Next to a deeper tissue penetration, a 2P excitation correlates with a reduced photodamage as well as enhanced spatial resolution. However, the Ru(II) polypyridine complexes reported so far were found to have relatively poor 2P photophysical properties^[7, 9a, 12] compared to porphyrins, porphyrin oligomers or expanded porphyrinoids,^[13] limiting the application of this technique with

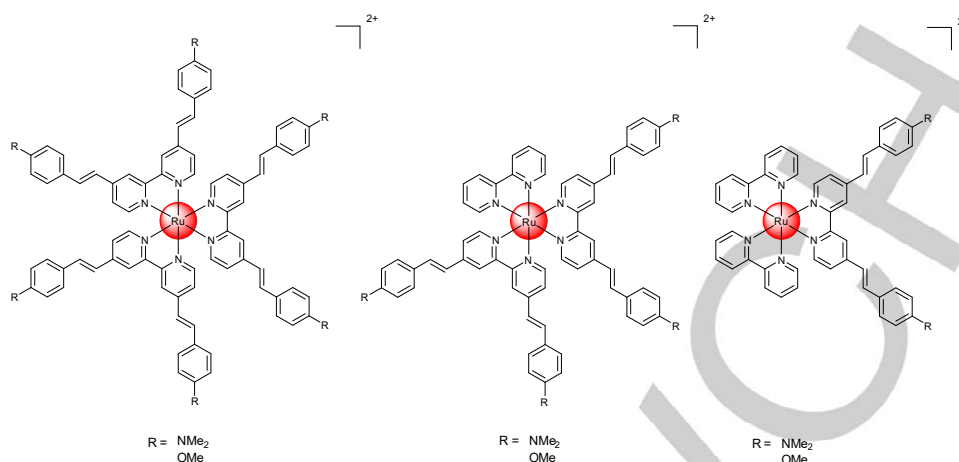
[a] Dr. J. Karges, Dr. Y. C. Ong, Dr. G. Gasser
Chimie ParisTech, PSL University, CNRS, Institute of Chemistry for Life and Health Sciences, Laboratory for Inorganic Chemical Biology, 75005 Paris, France.
gilles.gasser@chimieparistech.psl.eu; www.gassergroup.com

[b] S. Kuang, Prof. H. Chao
MOE Key Laboratory of Bioinorganic and Synthetic Chemistry, School of Chemistry, Sun Yat-Sen University, 510275 Guangzhou, People's Republic of China.
ceschh@mail.sysu.edu.cn

Supporting information for this article is given via a link at the end of the document.

RESEARCH ARTICLE

Previously studied compounds:



New compounds:

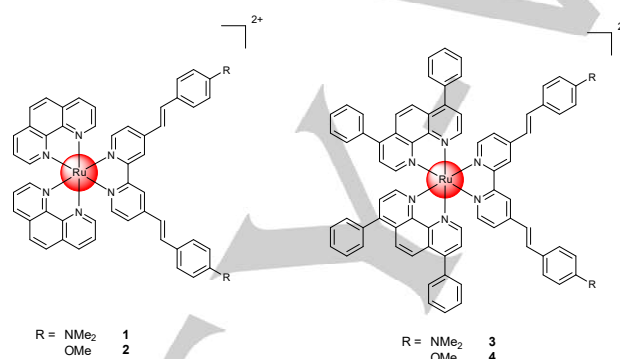


Figure 1. Chemical structures of previously studied and new compounds investigated in this work. The followed letter **a** corresponds to the compounds as a hexafluorophosphate salt whereas the letter **b** indicated the compound as a chloride salt.

these complexes. In this context, we have recently reported the rational design of the complexes $[\text{Ru}(\text{bipy})_n(\text{L-NMe}_2/\text{L-OMe})_{3-n}]^{2+}$ (bipy = 2,2'-bipyridine, L-NMe₂ = (*E,E*)-4,4'-bis[*p*-(*N,N*-dimethylamino)styryl]-2,2'-bipyridine, L-OMe = (*E,E*)-4,4'-bis[*p*-methoxystyryl]-2,2'-bipyridine, $n = 0, 1, 2$, Figure 1) as effective PSs for 1P (540 nm) and 2P (800 nm) PDT.^[14] Worthy of note, the use of (*E,E*)-4,4'-bisstyryl-2,2'-bipyridine type Ru(II) polypyridine complexes were previously reported as effective 2P absorbing chromophores.^[15] The lead compound of our study, namely $[\text{Ru}(\text{bipy})_2(\text{L-OMe})]^{2+}$ was found to be active *in vivo*.^[14] Despite the impressive biological property of this complex, its lack of 1P absorption in the biological spectral window and poor 2P absorption is limiting the application for deep-seated or large tumors.

With this in mind, in this work, the analogous complexes that bear different ancillary ligands $[\text{Ru}(\text{phen}/\text{bphen})_2(\text{L-NMe}_2/\text{L-OMe})]^{2+}$ (**1-4**, phen = 1,10-phenanthroline, bphen = 4,7-diphenyl-1,10-phenanthroline) are reported as effective PSs. The lead compound of this new study was found to have a red-shifted 1P and strong 2P absorption, enabling a phototherapeutic effect upon 1P (595 nm) or 2P (800 nm) excitation. An in-depth analysis of their ability to treat the hypoxic core in extraordinary large MCTS is presented. Further this complex was found to eradicate

an adenocarcinomic human alveolar basal epithelial tumour inside a mouse model.

Results and Discussion

To the best of our knowledge, the synthesis of the complexes **1-4** (Figure 1) has not been reported yet. The ligands L-NMe₂ and L-OMe were synthesized as previously reported by our group.^[14] The precursors $\text{Ru}(\text{phen})_2\text{Cl}_2$ and $\text{Ru}(\text{bphen})_2\text{Cl}_2$ were prepared as described in the literature.^[16] Finally, the chloride substituents of the respective precursors were substituted with L-NMe₂ or L-OMe, yielding the desired complexes **1a-4a**. All compounds were characterized using ¹H-, ¹³C-NMR, HR-MS analysis and the purity of the compounds verified by HPLC and elemental analysis. Details on the synthesis and characterization of the complexes can be found in the SI (Scheme S1-S2, Figure S1-S12).

To evaluate the potential of the compounds, their photophysical properties (Table S1) were determined. All complexes were found to have a strong red-shifted 1P absorption as indicated by their high extinction coefficients and absorption tail towards longer wavelengths (Figure S13a). Strikingly, the complexes have an exceptionally high 2P absorption up to ~1600 GM (Figure S13b), which is an order of magnitude higher than the majority of

RESEARCH ARTICLE

previously reported Ru(II) polypyridine complexes (~40-250 GM).^[7, 9a, 12] Importantly, the compounds have a 1P absorption tail towards and 2P absorption within the biological spectral window (600-900 nm), potentially allowing them to be utilized for the treatment of deep-seated or large tumours. The maximum of the emission of the complexes (Figure S14) was determined to be at 698 nm for the L-NMe₂-coordinated complexes (**1a**, **3a**) and at 663 nm for the L-OMe-coordinated complexes (**2a**, **4a**), resulting in a large Stokes shift for all investigated compounds. The comparison of the excitation and absorption spectra of all compounds showed no significant differences. The L-NMe₂ or L-OMe ligands play a significant role in the absorption and emission characteristics of the complexes since complexes **1** and **3** as well as **2a** and **4a** have similar absorption and emission profiles. The analysis of the excited states of the analogous bipy derivatives suggested that these transitions stem from metal-to-ligand charge transfer/ligand-to-metal charge transfer excitations.^[14] The comparison between the complexes revealed that the L-OMe-coordinated analogous (**2a**: 1.9 %, **4a**: 2.7 %) have a significantly higher luminescence quantum yield than the L-NMe₂-coordinated compounds (**1a**: 0.4 %, **3a**: 0.6 %). Worthy of note, other previously published Ru(II) polypyridine complexes with terminal dimethylamine groups were also found to be poorly luminescent.^[11c, 23d] Theoretical calculations for the [Ru(bphen)₂((*E,E*)-4,4'-bis(*N,N*-dimethylaminovinyl)-2,2'-bipyridine)]²⁺ complex indicated that the energetically lowest lying excitations are based on non-luminescent ligand-centred transitions.^[23d] The bphen coordinated compounds (**3a**, **4a**) showed a stronger luminescence than the phen coordinated compounds (**1a**, **2a**). This observation is in agreement with the comparison between the corresponding parent complexes [Ru(phen)₃]²⁺ and [Ru(bphen)₃]²⁺.^[17] All complexes were found to have excited state lifetimes in the nanosecond range (Figure S15-S18) in an aerated environment (i.e., 72-193 ns) and in a degassed environment (i.e., 334-981 ns). These values are in the same range than for other reported Ru(II) polypyridine complexes.^[18]

As the lifetimes drastically decrease in the presence of air, it indicates that the excited state can interact with a component of air. Capitalizing on this, the type of ROS generated upon light irradiation was then investigated by electron spin resonance spectroscopy using 2,2,6,6-tetramethylpiperidine as a singlet oxygen (¹O₂) scavenger and 5,5-dimethyl-1-pyrroline *N*-oxide as a [•]OOH or [•]OH radical scavenger. In contrast to the characteristic ¹O₂-induced triplet signal of 2,2,6,6-tetramethylpiperidinyloxy in CH₃CN and PBS for all complexes (Figure S19-S22), no significant signal was observed for the formation of [•]OOH or [•]OH radicals. The ¹O₂ quantum yields upon light exposure were determined using two complementary methods: 1) directly by measuring the phosphorescence signal of ¹O₂ upon excitation at 450 nm; 2) indirectly by capturing ¹O₂ with a reporter molecule and monitoring its change by absorbance spectroscopy upon excitation at 450 or 540 nm. The compounds (Table S2) were found to have ¹O₂ quantum yields in CH₃CN between 43-92 % and 2-14 % in an aqueous solution. The comparison between the compounds revealed that the ¹O₂ production of **2a** and **4a** is drastically higher than of **1a** and **3a**, which is expected due to their superior photophysical properties. The ¹O₂ generation of **2a** and **4a** is superior than their structurally related parent complexes

[Ru(phen)₃]²⁺ and [Ru(bphen)₃]²⁺ [17] as well as their analogous bipy derivatives.^[14]

The stability of a compound is a crucial factor in PDT applications. Previous studies have shown some metal complexes are not stable under physiological conditions, leading to undesired side effects.^[19] The compounds were incubated in human plasma at 37 °C and extracted after 48 h. No significant differences between the chromatograms (Figure S23-S26) were observed, indicating that all complexes were stable in a biological environment. Following this, the stability upon light exposure at 540 nm was investigated by monitoring their absorption spectra. Previous studies have shown that this could be an issue for some Ru(II) complexes.^[20] It is important to note that clinically used PSs, represented here by protoporphyrin IX (PpIX), are generally associated with a fast photodegradation.^[21] The compounds investigated in this study were found to be highly photostable (Figure S27-S30) whereas PpIX completely decomposed (Figure S31) under identical experimental conditions.

To study the effect that these complexes have on cells, we first assessed the time they need to be taken up by human cervical carcinoma (HeLa) cells using inductively coupled plasma mass spectrometry (ICP-MS). Within 6 h, the asymptotic maximum concentration (Figure S32-S35) was reached. The comparison between the complexes (Figure S36) shows that the bphen-coordinated complexes (**3a**, **4a**) are slightly better taken up by cells than the phen coordinated complexes (**1a**, **2a**). This result is in agreement with the determination of the log*P* values of the complexes (Table S3), which demonstrate their strong lipophilic character. Following this, the uptake mechanism of the compounds was investigated by blocking different pathways (Figure S37-S40) by preincubation with metabolic (2-deoxy-*D*-glucose and oligomycin), cationic transporter (tetraethylammonium chloride) and endocytotic (ammonium chloride or chloroquine) inhibitors as well as incubation at lower temperature (4 °C).^[22] As the incubation with tetraethylammonium chloride had only a negligible effect on the uptake, the internalization by this pathway was ruled out. The change to lower temperatures as well as the incubation with metabolic inhibitors significantly decreased the uptake, indicating that the mechanism is energy dependent. As the preincubation with ammonium chloride or chloroquine strongly decreased the internalization of the complexes **1a-4a**, it indicates that all compounds are taken up through an energy dependent endocytosis pathway. The subcellular localization was then examined using confocal laser scanning microscopy (Figure S41). The compounds were incubated in HeLa cells with commercial dyes for the major cellular organelles (i.e., nucleus, mitochondria, lysosomes, Golgi apparatus, endoplasmic reticulum) and their colocalization in the cells compared. As no significant overlap was observed, it suggests that the compounds do not majorly localize in these organelles. To further investigate the localization, the cell organelles were separately extracted and the amount of Ru determined by ICP-MS (Figure S42). All compounds were mainly found in the cytoplasm with small amounts of unselective accumulation. The structurally related bipy derivatives previously studied were also found to majorly localize in this organelle.^[14]

To study the (photo-)cytotoxic effects of **1a-4a**, these compounds were incubated in the dark as well as upon light exposure at 480 nm (10 min, 3.1 J/cm²) and 540 nm (40 min, 9.5 J/cm²) in non-

RESEARCH ARTICLE

cancerous retinal pigment epithelium (RPE-1), HeLa, mouse colon carcinoma (CT-26) and human glioblastoma astrocytoma (U373) cells. PpIX, the anticancer drug cisplatin and the parent complexes $[\text{Ru}(\text{phen})_3]^{2+}$ and $[\text{Ru}(\text{bphen})_3]^{2+}$ were used as controls. The light doses and irradiation times used in this work were optimized to the survival of the cells when treated only with the light source. All cell lines were tested identically to investigate the influence of the compounds on different types of cancer. The results (Table S4-S5) show that the phen-based compounds (**1a**, **2a**) as well as $[\text{Ru}(\text{phen})_3]^{2+}$ are non-toxic in the dark ($\text{IC}_{50} > 100$ μM), which is a crucial requirement for PDT applications. On the contrary, the bphen-coordinated complexes (**3a**, **4a**) were found to be cytotoxic in the low micromolar range ($\text{IC}_{50} = 5.2 - 20.8$ μM) in all tested cell lines. The observed cytotoxicity in the dark for the bphen-coordinated Ru(II) complexes could also be observed for $[\text{Ru}(\text{bphen})_3]^{2+}$ and is in agreement with recent studies of structurally related bphen-coordinated compounds.^[23] Upon light irradiation, all compounds were able to generate $^1\text{O}_2$, causing cell death in all investigated cell lines. The phen-coordinated compounds (**1a**, **2a**) were found to have a phototoxic effect in the low micromolar range ($\text{IC}_{50} = 0.9 - 15.6$ μM), while $[\text{Ru}(\text{phen})_3]^{2+}$ only had a negligible effect. The bphen-coordinated complexes (**3a**, **4a**) as well as $[\text{Ru}(\text{bphen})_3]^{2+}$ have, next to a cytotoxic effect in the dark, a phototoxic effect, as demonstrated by their IC_{50} values in the high nanomolar to low micromolar range ($\text{IC}_{50} = 0.5 - 2.1$ μM). The L-OMe-based compounds (**2a**, **4a**) were more phototoxic than the L-NMe₂-based compounds (**1a**, **3a**). This observation is attributed to their superior photophysical properties (Table S1-S2), notably their better $^1\text{O}_2$ production. Overall, **2a** was identified as the best compound of the series with no observed toxicity in the dark and a phototoxicity in the high nanomolar range in CT-26 cells ($\text{IC}_{50,540\text{nm}} = 0.9 \pm 0.4$ μM , $\text{PI}_{540\text{nm}} > 111$). These highly promising results of **2a** are an order of magnitude lower compared to the IC_{50} values of the PS PpIX, the parent complex $[\text{Ru}(\text{phen})_3]^{2+}$ and cisplatin tested under identical experimental conditions.

The phototoxic profile of the lead compound **2a** was further explored using longer wavelengths. **2a** was also active upon irradiation at 595 nm (60 min, 11.2 J/cm²) in CT-26 cells with an IC_{50} value in the low micromolar range ($\text{IC}_{50,595\text{nm}} = 2.4 \pm 0.3$ μM , $\text{PI}_{595\text{nm}} > 41.7$). In contrast, no phototoxicity was observed upon exposure to light at 620 nm (30 min, 3.3 J/cm²). The cell death mechanism caused upon irradiation at 480 nm (10 min, 3.1 J/cm²) was investigated by determining the cell viability upon preincubation with autophagy (3-methyladenine), apoptosis (Z-VAD-FMK), paraptosis (cycloheximide) and necrosis (necrostatin-1) inhibitors (Figure S43). Since preincubation with autophagy and necrosis inhibitors did not significantly influence the cell survival, these pathways were ruled out for all compounds. The preincubation with a paraptosis inhibitor slightly increased cell survival, while the preincubation with an apoptosis inhibitor highly increased cell survival. This indicates that the cell death is mainly caused by the apoptosis pathway, with minor contribution from the paraptosis pathway. Some previously studied PS were triggering cell death by the same mechanism.^[24] To further investigate the apoptosis mechanism, its dependency on caspases 3/7 was studied. Caspases 3/7 are well known executors of the intrinsic and extrinsic apoptosis mechanism.^[25] The caspase activity was measured in HeLa cells upon irradiation

at 480 nm (10 min, 3.1 J/cm²). The results show highly increased caspase levels upon irradiation (Figure S44), indicating that the phototoxic effect of all compounds is caused by a caspase 3/7 pathway. Some previously studied Ru(II) polypyridine complexes were found to exert their phototoxic effect by the same mechanism.^[26]

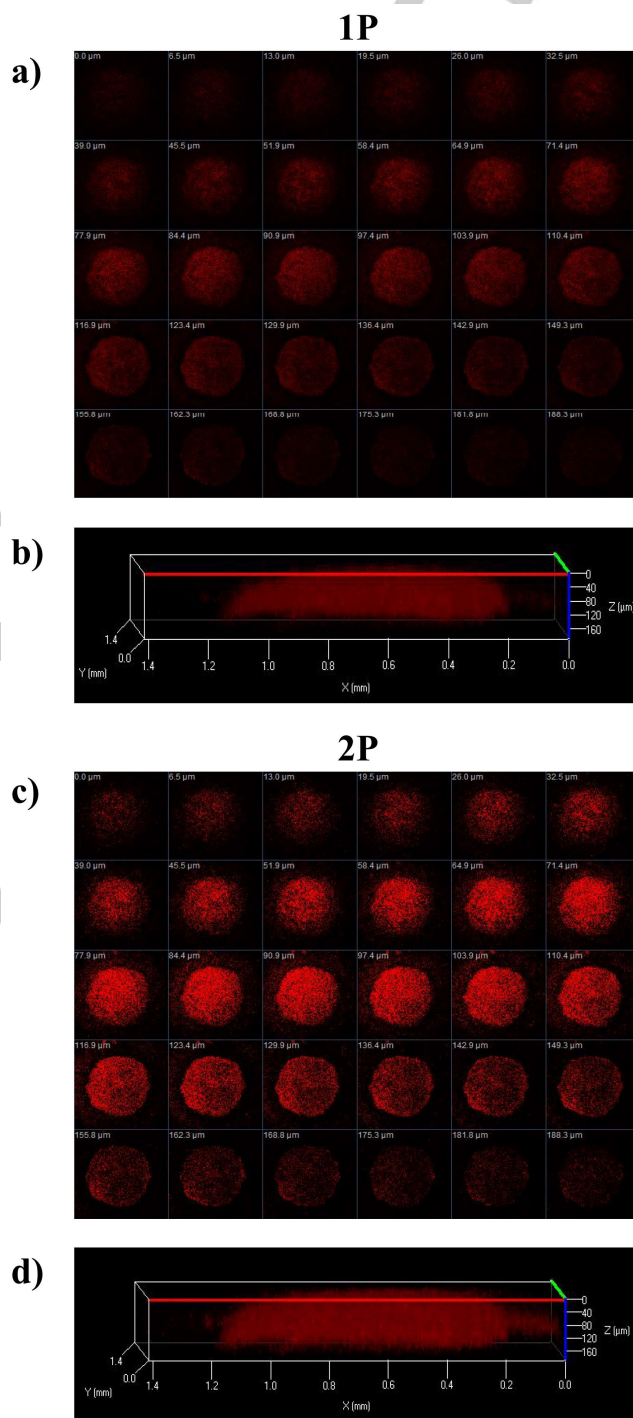


Figure 2. 1P ($\lambda_{\text{ex}} = 458$ nm, $\lambda_{\text{em}} = 600 - 750$ nm) and 2P ($\lambda_{\text{ex}} = 800$ nm, $\lambda_{\text{em}} = 600 - 750$ nm) excited Z-stack images in HeLa MCTS after incubation of **2a** (10 μM) for 12 h. **a/c**) Z-axis images scanning from the top to the bottom of an intact spheroid. **b/d**) 3D z-stack of an intact spheroid.

RESEARCH ARTICLE

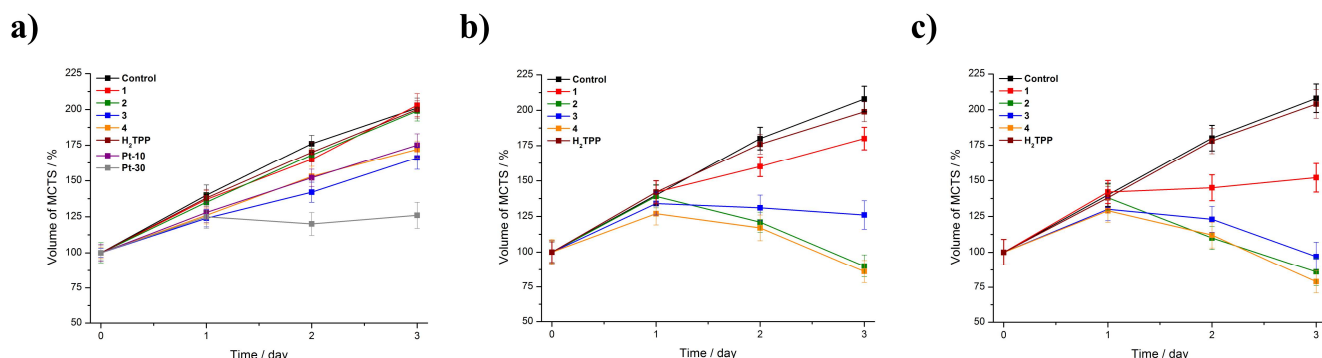


Figure 4. Tumour growth inhibition assay. Change of the volume in HeLa MCTSs in correlation to treatment time. The MCTSs were treated with the compounds **1a-4a** (20 μM), H_2TPP (20 μM) and cisplatin (10 μM and 30 μM). The MCTSs were **a)** strictly kept in the dark **b)** exposed to a 1P irradiation (500 nm, 10 J/cm^2) **c)** exposed to a 2P irradiation (800 nm, 10 J/cm^2 , section interval of 5 μm) on day 1. Representative pictures of the MCTSs can be found in Figure S48-S50. The error bars correspond to the standard deviation of the three replicates.

As a closer model to clinically treated cancer tumors, the biological effects of the compounds were evaluated in-depth in exceptionally large 3D multicellular tumour spheroids (MCTSs) with a diameter of 800 μm . In addition to the irradiation with a 1P light source, we have also studied their biological effect using a 2P light source. To investigate the penetration of the compounds inside the tumour model, HeLa MCTSs were incubated with **1a-4a** (10 μM) for 12 h and their 1P and 2P luminescence images by laser scanning confocal z-stack microscopy taken. Importantly, all compounds were able to fully penetrate the MCTSs up to their central cores, as demonstrated by the strong luminescence signal at every section depth (Figure 2, Figure S45-S47). A stronger luminescence signal following the 2P excitation in comparison to the 1P excitation was observed due to the deeper light penetration inside the MCTSs. Following this, the capacity of the compounds to generate $^1\text{O}_2$ upon irradiation inside the hypoxic centre of the MCTSs was investigated. For this purpose, HeLa MCTSs were incubated with 2',7-dichlorofluorescein diacetate (DCFH-DA), which is converted into the highly fluorescent 2',7-dichlorofluorescein in the presence of ROS. While no green fluorescence signal was observed in the dark, upon 2P irradiation (800 nm, 2 J/cm^2 , section interval of 5 μm), a strong signal in the whole MCTSs was detected (Figure 3). Strikingly, the signal was

also observed in the centre of the MCTSs, suggesting the generation of $^1\text{O}_2$ despite the hypoxic conditions, which are typically observed in MCTS.

To study the (photo-)cytotoxic effect in MCTSs, **1a-4a** (20 μM), cisplatin (10 μM and 30 μM) and the well-characterized PS tetraphenylporphyrin (H_2TPP , 20 μM) were exposed to 1P (500 nm, 10 J/cm^2) and 2P (800 nm, 10 J/cm^2 , section interval of 5 μm) irradiation and their tumour growth monitored (Figure 4). As observed in 2D monolayer cells, **3a** and **4a** showed a weak tumour growth inhibition effect in the dark similar to cisplatin at 10 μM while **1a** and **2a** did not significantly influence the tumour growth in the dark – the MCTSs grew in similar manner as the control. Upon 1P or 2P light treatment, all compounds **1a-4a** were able to cause a phototoxic effect inside the MCTSs leading to a decrease of the volume of the MCTSs. In particular, the compounds **2a** and **4a** drastically decreased the tumour growth upon light exposure, demonstrating their ability to act efficiently as a PS inside a 3D cellular architecture. Under identical conditions, the MCTSs treated with H_2TPP did not show any significant effects, highlighting the superior ability of these compounds.

To perform a deeper investigation of the phototoxic effect caused by the Ru(II) polypyridine complexes, the treated MCTSs were stained with calcein AM and propidium iodide to differentiate between living and dead cells. While the non-fluorescent calcein AM is converted to the highly green fluorescent calcein in living cells, propidium iodide is only able to penetrate dead cells with a damaged membrane integrity. It can then intercalate into DNA, causing a strong red fluorescence. As observed during the 2D monolayer screening, a significant dark cytotoxicity was detected for compounds **3a** and **4a**, while **1a** and **2a** showed no signs of cell death. Upon 1P or 2P irradiation, the vast majority of the MCTSs consisted of dead cells, as indicated by the strong red fluorescence signal of propidium iodide inside the MCTSs (Figure 5). Cellular damage was also caused in the large hypoxic centre, which remains so far a major challenge during a PDT treatment.

To further study and quantify the (photo-)cytotoxic effect of the complexes, their IC_{50} values in MCTSs in the dark as well as upon 1P (500 nm, 10 J/cm^2) and 2P (800 nm, 10 J/cm^2 , section interval of 5 μm) excitation were determined by measuring their ATP concentration. The obtained results (Table 1) are in agreement

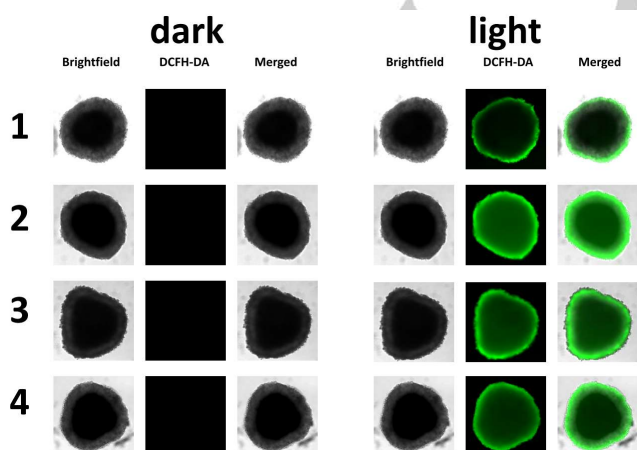


Figure 3. Confocal fluorescent images of HeLa MCTSs incubated with DCFH-DA and the compounds **1a-4a** (2 μM) kept in the dark and after a 2P irradiation (800 nm, 2 J/cm^2 , section interval of 5 μm).

RESEARCH ARTICLE

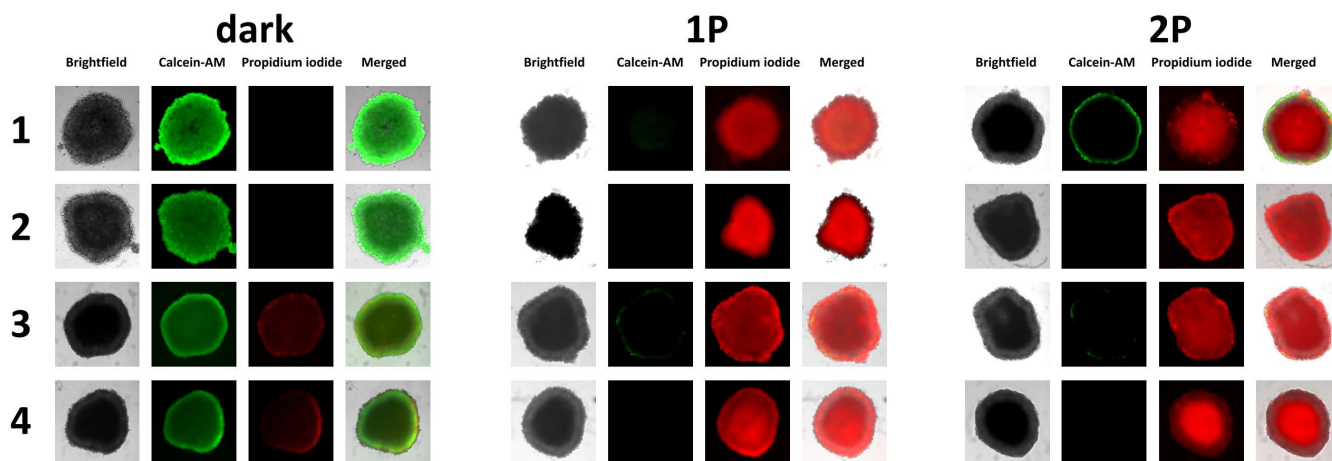


Figure 5. Representative image of the viability assay with HeLa MCTSs kept in the dark and exposed to light. MCTS were treated with the compounds **1-4** (20 μM) in the dark for 12 h. After this time, MCTSs were exposed to a 1P (500 nm, 10 J/cm^2) or a 2P irradiation (800 nm, 10 J/cm^2 , section interval of 5 μm). After 2 days, the cell survival was assessed by measurement of the fluorescence of calcein ($\lambda_{\text{ex}} = 495 \text{ nm}$, $\lambda_{\text{em}} = 515 \text{ nm}$) and cell death by measurement of the fluorescence of propidium iodide ($\lambda_{\text{ex}} = 536 \text{ nm}$, $\lambda_{\text{em}} = 617 \text{ nm}$).

with the tumour growth inhibition assay, showing that the bphen-coordinated complexes (**3a**, **4a**) have a cytotoxic effect in the low micromolar range in the dark while the phen-coordinated complexes (**1a**, **2a**) showed no dark toxicity even up to high micromolar range ($\text{IC}_{50} > 300 \mu\text{M}$). Upon exposure to 1P or 2P irradiation, all compounds were able to cause a phototoxic effect in the micromolar range ($\text{IC}_{50,1\text{P}} = 3.8 - 32.6 \mu\text{M}$, $\text{IC}_{50,2\text{P}} = 0.8 - 27.8 \mu\text{M}$). As the lead compound of this study, **2a** demonstrated its remarkable ability as a PS with PI values of >40 upon 1P and >250 upon 2P irradiation. Further, **2a** was also found to be phototoxic in HeLa MCTSs upon irradiation at 595 nm (60 min, 11.2 J/cm^2) in the low micromolar range ($\text{IC}_{50,595\text{nm}} = 16.7 \pm 1.2 \mu\text{M}$, $\text{PI}_{595\text{nm}} > 18$). Overall, the lead compound **2** was found to have a two order of magnitudes higher phototoxicity in comparison to H_2TTP , indicating that the compounds reported here can act using very low drug and light doses.

Table 1. IC_{50} values in the dark as well as upon 1P (500 nm, 10 J/cm^2) and 2P (800 nm, 10 J/cm^2 , section interval of 5 μm) irradiation of **1a-4a** as well as of cisplatin and H_2TTP in HeLa 3D MCTS. Average of three independent measurements. n.d. = not determinable.

	dark	1P	PI	2P	PI
1	>300	32.6 ± 2.5	>9.2	27.8 ± 3.1	>10.8
2	>300	7.5 ± 0.2	>40.0	1.2 ± 0.3	>250.0
3	27.8 ± 3.6	8.9 ± 0.7	3.1	3.1 ± 0.6	9.0
4	29.3 ± 2.9	3.8 ± 0.4	7.7	0.8 ± 0.5	36.6
H_2TTP	>100	>100	n.d.	>100	n.d.
cisplatin	18.6 ± 1.3	-	-	-	-

For a further investigation, the biological properties of **2** inside a mouse model was investigated. As the counter ion of a metal complex can have a significant effect on the overall ability of the compound including its water solubility or toxicity^[27], **2a** was converted into the chloride salt **2b** using a counter ion exchange resin. The biodistribution of the compound inside of nude mice bearing an adenocarcinomic human alveolar basal epithelial (A549) tumour upon intravenous tail-injection was time-dependently (0.5, 1, 2, 4 h) studied. At each time point, the mice were sacrificed, all major organs collected (i.e., blood, spleen, intestine, gastric, liver, kidney, lung, heart, brain, tumour), ground

and the amount of Ru inside each organ determined by ICP-MS (Figure S51). The compound was rapidly absorbed from the blood stream, accumulating mainly within the liver and kidney. The compound also accumulated inside the tumour with a concentration maximum 2 h after the injection. Capitalizing on these results, *in vivo* PDT experiments were performed using a 1P (500 nm, 10 mW/cm^2 , 15 min) or 2P irradiation (800 nm, 50 mW , 1 kHz, pulse width 35 fs, 5 s/mm) light treatment on days 1, 4 and 7. Encouragingly, the PDT treated tumours drastically shrank until they were nearly eradicated. It is important to mention that while the tumours treated with a 2P light source did not show a significant growth after the treatment, the tumours treated with a 1P light source did indicate a small tumour growth. We assume that this could be caused by the deeper light tissue penetration of 2P irradiation compared to 1P. In contrast, the tumours only treated by light or with the compound did not show any tumour inhibition effect (Figures 6a and 6c). The animals treated with the compound behaved normally, without signs of pain, stress or discomfort and did not lose or gain weight (Figure 6b). After 17 days (representative picture: Figure S52), all mice were sacrificed and the tumour and organs separated. As expected, using a histological examination with an H&E stain the tumour tissue showed noticeable pathological alterations (Figure S53) while all major organs did not show any pathological effect (Figure S54).

RESEARCH ARTICLE

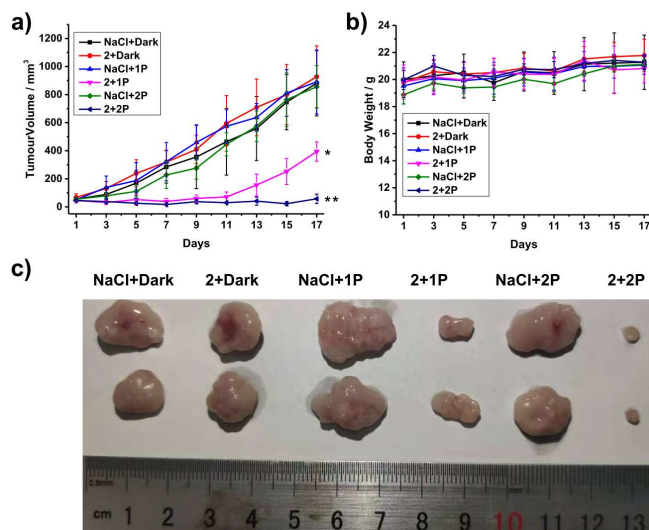


Figure 6. *In vivo* PDT study of **2b** using 1P (500 nm, 10 mW/cm², 15 min) or 2P (800 nm, 50 mW, 1 kHz, pulse width 35 fs, 5 s/mm) excitation on nude mice bearing an adenocarcinomic human alveolar basal epithelial cancer tumour. **a)** Tumour growth inhibition curves upon treatment. **b)** Average body weights of the tumour-bearing mice. **c)** Representative photographs of the tumour after different treatments on day 17. **p*<0.05, ***p*<0.01.

Conclusion

In summary, a series of new asymmetric substituted 1,10-phenanthroline and 4,7-diphenyl-1,10-phenanthroline Ru(II) polypyridine complexes is presented as efficient PSs for 1- and 2-Photon PDT. The complexes showed a red shifted 1-Photon absorption towards and exceptionally strong 2-Photon absorption in the biological spectral window. They were found to enter cells by an energy dependent endocytosis mechanism, where the complexes accumulated primarily in the cytoplasm. Upon irradiation in various 2D monolayer cancer cell lines, the complexes caused cell death in the high nanomolar/low micromolar range by apoptosis utilising the caspase 3/7 pathway. Following this, the efficiency of the compounds was investigated in exceptionally large MCTSs with a diameter of 800 μm, which can better simulate the pathological conditions found in clinically-relevant tumours. All complexes were able to fully penetrate the MCTSs and to generate singlet oxygen in their hypoxic centres. Strikingly, after the treatment, the MCTSs were fully eradicated, including in their large hypoxic centres. While the lead compound of this study, **2** was found to be non-toxic in the dark, it is highly phototoxic in MCTSs in the very low micromolar range upon 1-Photon (595 nm) or 2-Photon (800 nm) irradiation. Worthy of note, in comparison to the previously published 2,2'-bipyridine analogous compounds, these complexes were found to be photoactive upon even longer wavelengths by 1-Photon irradiation. In addition, **2** was also able to eradicate an adenocarcinomic human alveolar basal epithelial tumour inside a mouse model upon clinically relevant 1-Photon (500 nm) or 2-Photon (800 nm) excitation, demonstrating its high potential as a PS. Overall, the compounds presented in this study can overcome the limitations of currently applied PSs. We strongly believe that these complexes, especially **2**, has great potential for 1- and 2-

Photon excited PDT and is a suitable candidate for further clinical investigations.

Acknowledgements

We thank Dr. Philippe Goldner for access to state-of-the-art laser apparatus. This work was financially supported by an ERC Consolidator Grant PhotoMedMet to G.G. (GA 681679), has received support under the program "Investissements d' Avenir" launched by the French Government and implemented by the ANR with the reference ANR-10-IDEX-0001-02 PSL (G.G.), the National Science Foundation of China (Nos. 21525105 and 21778079 for H.C.) and the 973 Program (No. 2015CB856301 for H.C.).

Author Contributions: J. K., S. K., H. C. and G. G. were involved with the design and interpretation of experiments and with the writing of the manuscript. Chemical, photophysical and biological cellular experiments were carried out by J.K. Animal testing was carried out by S. K. Comments on the English writing style were provided by Y. C. O. The work was supervised by H. C. and G. G. All authors have given approval to the final version of the manuscript.

Keywords: Bioinorganic Chemistry • Medicinal Inorganic Chemistry • Metals in Medicine • Photodynamic Therapy • Photosensitizers

- [1] a)S. Bonnet, *Dalton Trans.* **2018**, 47, 10330-10343; b)S. Callaghan, M. O. Senge, *Photochem. Photobiol. Sci.* **2018**, 17, 1490-1514; c)P.-C. Lo, M. S. Rodríguez-Morgade, R. K. Pandey, D. K. P. Ng, T. Torres, F. Dumoulin, *Chem. Soc. Rev.* **2020**, 49, 1041-1056; d)F. Heinemann, J. Karges, G. Gasser, *Acc. Chem. Res.* **2017**, 50, 2727-2736.
- [2] B. Muz, P. de la Puente, F. Azab, A. K. Azab, *Hypoxia* **2015**, 3, 83-92.
- [3] a)C. A. Robertson, D. H. Evans, H. Abrahamse, *J. Photochem. Photobiol. B.* **2009**, 96, 1-8; b)S. Mallidi, S. Anbil, A.-L. Bulin, G. Obaid, M. Ichikawa, T. Hasan, *Theranostics* **2016**, 6, 2458-2487; c)C. Imberti, P. Zhang, H. Huang, P. J. Sadler, *Angew. Chem. Int. Ed.*, **2020**, 59, 61-73; d)F. Dumoulin, *Photodiagnosis Photodyn. Ther.* **2017**, 17, A4 - A78.
- [4] a)R. M. Sutherland, *Science* **1988**, 240, 177-184; b)P. A. Netti, D. A. Berk, M. A. Swartz, A. J. Grodzinsky, R. K. Jain, *Cancer Res.* **2000**, 60, 2497-2503; c)S. Riffle, R. S. Hegde, *J. Exp. Clin. Cancer Res.* **2017**, 36, 102-112; d)P. J. Dyson, *Natl. Sci. Rev.* **2019**, 6, 1068-1069.
- [5] a)L. A. Kunz-Schughart, *Cell Biol. Int.* **1999**, 23, 157-161; b)J. Friedrich, C. Seidel, R. Ebner, L. A. Kunz-Schughart, *Nat. Protoc.* **2009**, 4, 309-324
- [6] a)I. Freitas, *Tumori J.* **1985**, 71, 251-259; b)M. Höckel, P. Vaupel, *J. Natl. Cancer Inst.* **2001**, 93, 266-276; c)L. N. Lameijer, D. Ernst, S. L. Hopkins, M. S. Meijer, S. H. C. Askes, S. E. Le Dévédec, S. Bonnet, *Angew. Chem. Int. Ed.* **2017**, 56, 11549-11553; d)J. Fong, K. Kasimova, Y. Arenas, P. Kaspler, S. Lazic, A. Mandel, L. Lilge, *Photochem. Photobiol. Sci.* **2015**, 14, 2014-2023; e)P. Zhang, P. J. Sadler, *Eur. J. Inorg. Chem.* **2017**, 2017,

RESEARCH ARTICLE

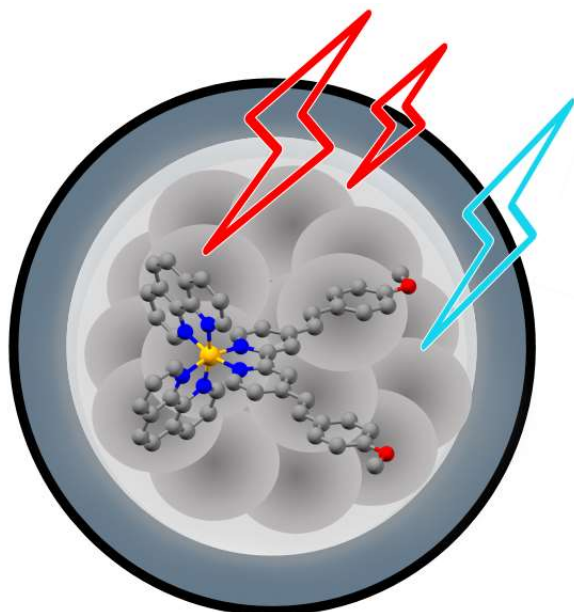
- 1541-1548; f)H. Huang, S. Banerjee, K. Qiu, P. Zhang, O. Blacque, T. Malcomson, M. J. Paterson, G. J. Clarkson, M. Staniforth, V. G. Stavros, G. Gasser, H. Chao, P. J. Sadler, *Nat. Chem.* **2019**, *11*, 1041-1048; g)J. Roque III, D. Havrylyuk, P. C. Barrett, T. Sainuddin, J. McCain, K. Colón, W. T. Sparks, E. Bradner, S. Monro, D. Heidary, C. G. Cameron, E. C. Glazer, S. A. McFarland, *Photochem. Photobiol.* **2019**, *2*, 327-339
- [7] A. Raza, S. A. Archer, S. D. Fairbanks, K. L. Smitten, S. W. Botchway, J. A. Thomas, S. MacNeil, J. W. Haycock, *J. Am. Chem. Soc.* **2020**, *142*, 4639-4647.
- [8] a)D. R. Grimes, C. Kelly, K. Bloch, M. Partridge, *J. R. Soc. Interface* **2014**, *11*, 20131124; b)W. R. Wilson, M. P. Hay, *Nat. Rev. Cancer* **2011**, *11*, 393-410.
- [9] a)H. Huang, B. Yu, P. Zhang, J. Huang, Y. Chen, G. Gasser, L. Ji, H. Chao, *Angew. Chem. Int. Ed.* **2015**, *54*, 14049-14052; b)B. S. Howerton, D. K. Heidary, E. C. Glazer, *J. Am. Chem. Soc.* **2012**, *134*, 8324-8327; c)V. H. S. van Rixel, V. Ramu, A. B. Auyeung, N. Beztsinna, D. Y. Leger, L. N. Lameijer, S. T. Hilt, S. E. Le Dévédec, T. Yildiz, T. Betancourt, M. B. Gildner, T. W. Hudnall, V. Sol, B. Liagre, A. Kornienko, S. Bonnet, *J. Am. Chem. Soc.* **2019**, *141*, 18444-18454.
- [10] a)R. Lincoln, L. Kohler, S. Monro, H. Yin, M. Stephenson, R. Zong, A. Chouai, C. Dorsey, R. Hennigar, R. P. Thummel, S. A. McFarland, *J. Am. Chem. Soc.* **2013**, *135*, 17161-17175; b)A. M. Palmer, B. Peña, R. B. Sears, O. Chen, M. E. Ojaimi, R. P. Thummel, K. R. Dunbar, C. Turro, *Philos. Trans. R. Soc. A* **2013**, *371*, 20120135; c)J. Yellol, S. A. Pérez, A. Buceta, G. Yellol, A. Donaire, P. Szumlas, P. J. Bednarski, G. Makhoulfi, C. Janiak, A. Espinosa, J. Ruiz, *J. Med. Chem.* **2015**, *58*, 7310-7327; d)F. E. Poynton, S. A. Bright, S. Blasco, D. C. Williams, J. M. Kelly, T. Gunnlaugsson, *Chem. Soc. Rev.* **2017**, *46*, 7706-7756; e)A. Li, C. Turro, J. J. Kodanko, *Acc. Chem. Res.* **2018**, *51*, 1415-1421; f)R. F. Brissos, P. Clavero, A. Gallen, A. Grabulosa, L. A. Barrios, A. B. Caballero, L. Korrodi-Gregório, R. Pérez-Tomás, G. Muller, V. Soto-Cerrato, P. Gamez, *Inorg. Chem.* **2018**, *57*, 14786-14797; g)J. Shum, P. K.-K. Leung, K. K.-W. Lo, *Inorg. Chem.* **2019**, *58*, 2231-2247; h)J. Karges, F. Heinemann, F. Maschietto, M. Patra, O. Blacque, I. Ciofini, B. Spingler, G. Gasser, *Biorg. Med. Chem.* **2019**, *27*, 2666-2675; i)S. Monro, K. L. Colón, H. Yin, J. Roque III, P. Konda, S. Gujar, R. P. Thummel, L. Lilge, C. G. Cameron, S. A. McFarland, *Chem. Rev.* **2019**, *119*, 797-828; j)M. S. Meijer, S. Bonnet, *Inorg. Chem.* **2019**, *58*, 11689-11698; j)P. J. Jarman, F. Noakes, S. Fairbanks, K. Smitten, I. K. Griffiths, H. K. Saeed, J. A. Thomas, C. Smythe, *J. Am. Chem. Soc.* **2019**, *141*, 2925-2937; k)J. Karges, T. Yempala, M. Tharaud, D. Gibson, G. Gasser, *Angew. Chem.* **2020**, *59*, 7069-7075 ; l)N. Soliman, L. K. McKenzie, J. Karges, E. Bertrand, M. Tharaud, M. Jakubaszek, V. Guérineau, B. Goud, M. Hollenstein, G. Gasser, C. M. Thomas, *Chem. Sci.* **2020**, *11*, 2657-2663; m)N. P. Toupin, S. Nadella, S. J. Steinke, C. Turro, J. J. Kodanko, *Inorg. Chem.* **2020**, *59*, 3919-3933.
- [11] a)P. Kaspler, S. Lazic, S. Forward, Y. Arenas, A. Mandel, L. Lilge, *Photochem. Photobiol. Sci.* **2016**, *15*, 481-495; b)V. Novohradsky, A. Rovira, C. Hally, A. Galindo, G. Viguera, A. Gandioso, M. Svitelova, R. Bresolí-Obach, H. Kosthunova, L. Markova, J. Kasparkova, S. Nonell, J. Ruiz, V. Brabec, V. Marchán, *Angew. Chem. Int. Ed.* **2019**, *58*, 6311-6315; c)J. Karges, O. Blacque, P. Goldner, H. Chao, G. Gasser, *Eur. J. Inorg. Chem.*, **2019**, *2019*, 3704-3712; d)D. Havrylyuk, K. Stevens, S. Parkin, E. C. Glazer, *Inorg. Chem.* **2020**, *59*, 1006-1013.
- [12] a)C. Girardot, G. Lemerrier, J. C. Mulatier, J. Chauvin, P. L. Baldeck, C. Andraud, *Dalton Trans.* **2007**, 3421-3426; b)S. C. Boca, M. Four, A. Bonne, B. Van Der Sanden, S. Astilean, P. L. Baldeck, G. Lemerrier, *Chem. Commun.* **2009**, 4590-4592; c)J. Liu, Y. Chen, G. Li, P. Zhang, C. Jin, L. Zeng, L. Ji, H. Chao, *Biomaterials* **2015**, *56*, 140-153; d)L. Zeng, S. Kuang, G. Li, C. Jin, L. Ji, H. Chao, *Chem. Commun.* **2017**, *53*, 1977-1980; e)K. Qiu, J. Wang, C. Song, L. Wang, H. Zhu, H. Huang, J. Huang, H. Wang, L. Ji, H. Chao, *ACS Appl. Mater. Interfaces* **2017**, *9*, 18482-18492; f)J. Hess, H. Huang, A. Kaiser, V. Pierroz, O. Blacque, H. Chao, G. Gasser, *Chem. Eur. J.* **2017**, *41*, 9888-9896.
- [13] a)M. Drobizhev, Y. Stepanenko, Y. Dzenis, A. Karotki, A. Rebane, P. N. Taylor, H. L. Anderson, *J. Phys. Chem. B* **2005**, *109*, 7223-7236; b)T. K. Ahn, K. S. Kim, D. Y. Kim, S. B. Noh, N. Aratani, C. Ikeda, A. Osuka, D. Kim, *J. Am. Chem. Soc.* **2006**, *128*, 1700-1704; c)M.-C. Yoon, S. B. Noh, A. Tsuda, Y. Nakamura, A. Osuka, D. Kim, *J. Am. Chem. Soc.* **2007**, *129*, 10080-10081; d)M. Pawlicki, H. A. Collins, R. G. Denning, H. L. Anderson, *Angew. Chem. Int. Ed.* **2009**, *48*, 3244-3266.
- [14] J. Karges, S. Kuang, F. Maschietto, O. Blacque, I. Ciofini, H. Chao, G. Gasser, *Nat. Commun.* **2020**, *11*, 3262.
- [15] a)C. Feuvrie, O. Maury, H. Le Bozec, I. Ledoux, J. P. Morrall, G. T. Dalton, M. Samoc, M. G. Humphrey, *J. Phys. Chem. A* **2007**, *111*, 8980-8985; b)M. G. Humphrey, T. Schwich, P. J. West, M. P. Cifuentes, M. Samoc, *Comprehensive Inorganic Chemistry II* (Second Edition) (Eds.: J. Reedijk, K. Poeppelemeier), Elsevier, Amsterdam, **2013**, 781-835.
- [16] B. P. Sullivan, D. J. Salmon, T. J. Meyer, *Inorg. Chem.* **1978**, *17*, 3334-3341.
- [17] D. Garcia-Fresnadillo, Y. Georgiadou, G. Orellana, A. M. Braun, E. Oliveros, *Helv. Chim. Acta* **1996**, *79*, 1222-1238.
- [18] a)M. J. Cook, A. P. Lewis, G. S. McAuliffe, V. Skarda, A. J. Thomson, J. L. Glasper, D. J. Robbins, *J. Chem. Soc., Perkin Trans. 2* **1984**, 1293-1301; b)V. Balzani, A. Juris, *Coord. Chem. Rev.* **2001**, *211*, 97-115.
- [19] a)M. D. Hall, K. A. Telma, K.-E. Chang, T. D. Lee, J. P. Madigan, J. R. Lloyd, I. S. Goldlust, J. D. Hoeschele, M. M. Gottesman, *Cancer Res.* **2014**, *74*, 3913-3922; b)S. Keller, Y. C. Ong, Y. Lin, K. Cariou, G. Gasser, *J. Organomet. Chem.* **2019**, 121059;
- [20] a)U. Basu, J. Karges, F. Chotard, C. Balan, P. Le Gendre, G. Gasser, E. Bodio, R. Malacea Kabbara, *Polyhedron* **2019**, *172*, 22-27; b)A. K. Renfrew, J. Karges, R. Scopelliti, F. D. Bobbink, P. Nowak-Sliwinska, G. Gasser, P. Dyson, *ChemBioChem* **2019**, *20*, 2876-2882.
- [21] a)T. S. Mang, T. J. Dougherty, W. R. Potter, D. G. Boyle, S. Somer, J. Moan, *Photochem. Photobiol.* **1987**, *45*, 501-506; b)J. Moan, G. Streckyte, S. Bagdonas, Ø. Bech, K. Berg, *Int. J. Cancer* **1997**, *70*, 90-97.
- [22] a)J. Karges, U. Basu, O. Blacque, H. Chao, G. Gasser, *Angew. Chem. Int. Ed.*, **2019**, *58*, 14334-14340; b)J. Karges, O. Blacque, H. Chao, G. Gasser, *Inorg. Chem.* **2019**, *58*, 12422-12432.
- [23] a)C. Tan, S. Wu, S. Lai, M. Wang, Y. Chen, L. Zhou, Y. Zhu, W. Lian, W. Peng, L. Ji, A. Xu, *Dalton Trans.* **2011**, *40*, 8611-8621; b)M. R. Gill, D. Cecchin, M. G. Walker, R. S. Mulla, G. Battaglia, C. Smythe, J. A. Thomas, *Chem. Sci.* **2013**, *4*, 4512-4519; c)M. Dickerson, Y. Sun,

RESEARCH ARTICLE

- B. Howerton, E. C. Glazer, *Inorg. Chem.* **2014**, *53*, 10370-10377; d)H. Audi, D. Azar, F. Mahjoub, S. Farhat, Z. El-Masri, M. El-Sibai, R. J. Abi-Habib, R. S. Khnayzer, *J. Photochem. Photobiol. A* **2018**, *351*, 59-68; d)J. Karges, F. Heinemann, M. Jakubaszek, F. Maschietto, C. Subecz, M. Dotou, O. Blacque, M. Tharaud, B. Goud, E. V. Zahinos, B. Spingler, I. Ciofini, G. Gasser, *J. Am. Chem. Soc.* **2020**, *142*, 6578–6587.
- [24] a)V. H. S. van Rixel, B. Siewert, S. L. Hopkins, S. H. C. Askes, A. Busemann, M. A. Siegler, S. Bonnet, *Chem. Sci.* **2016**, *7*, 4922-4929; b)D. Kessel, *Photochem. Photobiol.* **2019**, *95*, 119-125; c)V. Rapozzi, F. D'Este, L. E. Xodo, *J. Porphyr. Phthalocyanines* **2019**, *23*, 410-418; d)C. Donohoe, M. O. Senge, L. G. Arnaut, L. C. Gomes-da-Silva, *Biochim. Biophys. Acta* **2019**, *1872*, 188308; e)N. M. Vegi, S. Chakraborty, M. M. Zegota, S. L. Kuan, A. Stumper, V. P. S. Rawat, S. Sieste, C. Buske, S. Rau, T. Weil, M. Feuring-Buske, *Sci. Rep.* **2020**, *10*, 371.
- [25] J. M. Adams, *Genes Dev.* **2003**, *17*, 2481-2495.
- [26] a)C. Qian, J.-Q. Wang, C.-L. Song, L.-L. Wang, L.-N. Ji, H. Chao, *Metallomics* **2013**, *5*, 844-854; b)H. Huang, P. Zhang, B. Yu, Y. Chen, J. Wang, L. Ji, H. Chao, *J. Med. Chem.* **2014**, *57*, 8971-8983.
- [27] a)E. A. Thackaberry, *Expert Opin. Drug Metab. Toxicol.* **2012**, *8*, 1419-1433; b)B.-Z. Zhu, X.-J. Chao, C.-H. Huang, Y. Li, *Chem. Sci.* **2016**, *7*, 4016-4023.

RESEARCH ARTICLE

Entry for the Table of Contents



The treatment of large cancer tumours with photodynamic therapy (PDT) remains a major medical challenge due to the problems of the photosensitizers (PSs) to penetrate a 3D cellular structure and the low oxygen concentrations available in the tumor centre. Herein, a series of Ru(II) polypyridine complexes is presented as PSs for 1- and 2-Photon PDT for the treatment of the hypoxic centre of exceptionally large multicellular tumour spheroids.

Institute and/or researcher Twitter usernames:

Johannes Karges: @Johannes_Karges

Gilles Gasser: @GasserGroup

Universite PSL: @psl_univ